Korean J. Chem. Eng., 38(6), 1161-1169 (2021)
DOI: 10.1007/s11814-021-0752-1

pISSN: 0256-1115
eISSN: 1975-7220

Cascade conversion of glucose to 5-hydroxymethylfurfural over Brönsted-Lewis bi-acidic SnAl-beta zeolites

Hyejin An*, Sungjoon Kweon*, Dong-Chang Kang, Chae-Ho Shin**, Jeong F. Kim*, Min Bum Park*,†, and Hyung-Ki Min***,†**

*Department of Energy and Chemical Engineering, Incheon National University, Incheon 22012, Korea
**Department of Chemical Engineering, Chungbuk National University, Cheongju, Chungbuk 28644, Korea
***LOTTE Chemical Research Institute, Daejeon 34110, Korea
(*Received 14 November 2020 • Revised 1 January 2021 • Accepted 26 January 2021*)

Abstract−The control of acidic properties in a catalyst is one of the key features of technology utilizing biomass for chemical production. In this study, the Brönsted and Lewis bi-acidic SnAl-beta zeolites with controllable acidity were successfully prepared by acid dealumination and isomorphic substitution of Al by Sn, and applied for the cascade conversion of glucose to 5-hydroxymethylfurfural (5-HMF). The Lewis acidity of the catalysts was increased as the higher concentration of nitric acid used for the dealumination process. The optimum portion of Lewis/(Brönsted+Lewis) ratio was investigated to maximize the yield of 5-HMF, which is converted from the glucose via fructose by the cascade reaction. The conversion of glucose was increased until the L/(B+L) ratio reached 0.89 and the selectivity to 5-HMF reached its maximum at the Lewis acid portion of 0.76 among the total acid sites.

Keywords: Beta Zeolite, Glucose Conversion, Cascade Reaction, 5-Hydroxymethylfurfural, Bi-acidic Catalysts

INTRODUCTION

Biomass-derived carbohydrates are potential raw materials of chemical industry alternative to the fossil fuels, which are responsible for carbon dioxide emission. Carbohydrates are the most abundant component (ca. 75%) in biomass and their use as chemical feedstocks is carbon neutral because they originate from carbon dioxide and water through photosynthesis. There have been numerous trials to utilize carbohydrates as a chemical feedstock, e.g., ethylene glycol, propylene glycol, acrylates, and furan derivatives [1,2]. Among the various carbohydrates, glucose is the most abundant and inexpensive starting material for the production of a variety of platform chemicals, such as 5-hydroxymethylfurfural (5-HMF), sorbitol, gluconic acid, succinic acid, levulinic acid, and butanediol [3-6]. 5-HMF, a kind of furan derivative obtained from glucose or fructose, is a representative chemical building block that is utilized for the replacement of formaldehyde in resins, adhesives, and coatings, for the precursor of furan-2,5-dicarboxylic acid (FDCA) and its polymer (polyethylene furanoate, PEF), and for the active natural ingredient in nutraceuticals and dietary foods [7].

Glucose conversion to 5-HMF proceeds via a two-step cascade reaction, involving isomerization of glucose to fructose over Lewis acid catalysts and dehydration of fructose to 5-HMF over Brönsted acids, is shown in Scheme 1. Up to now, many types of cata-

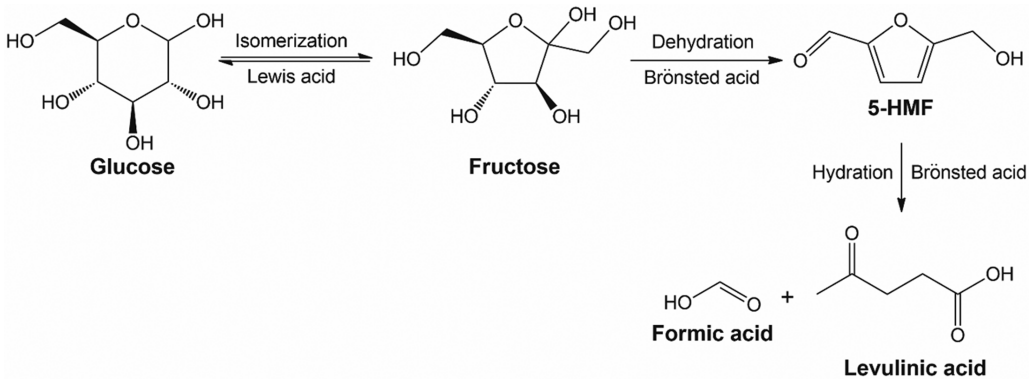

Scheme 1. Cascade conversion of glucose to 5-HMF over Brönsted and Lewis acid catalysts.

†To whom correspondence should be addressed.
E-mail: mbpark@inu.ac.kr, pulcherrima7@gmail.com

lysts, e.g., metal oxides, zeolites, mesoporous silica, and heteropoly acid having bi-acidic properties, were employed for the conversion of glucose to 5-HMF [8]. In the cascade conversion of glucose to 5-HMF, the balance between Lewis and Brönsted acid in the catalyst is important to avoid undesired side reactions (e.g., the formation of levulinic and formic acids by 5-HMF hydration). Zhang et al. employed the ZrO_2 catalyst with balanced Lewis and Brönsted acid sites by optimizing calcination temperature, and reported 5-HMF yield of 40% [9]. Yan and co-workers impregnated SO_4^{2-} ion on ZrO_2-Al_2O_3 to increase the acidity of catalysts and obtained optimized 5-HMF yield of 48% [10]. Chung et al. reported high yield (50%) of 5-HMF over bi-functional Cu-Cr/ZSM-5 zeolite catalyst (framework type MFI) due to the increase of acidity by metal ion addition [11]. Swift et al. showed that the higher Lewis/Brönsted ratio was beneficial for the formation of 5-HMF when using H-beta (*BEA) zeolite catalysts [12]. On the other hand, Hu and co-workers compared the catalytic activity of various zeolites with different framework types (i.e., FAU, MOR, MFI, and *BEA) and found the highest 5-HMF yield (50%) of H-beta zeolite over other structures [13]. In addition, a tin (Sn)-containing mesoporous silica (Sn-MCM-41) was synthesized as the bi-functional heterogeneous catalyst for the conversion of glucose and the 5-HMF yield reached up to 70% at 110 °C [14].

Zeolite beta is one of the most complex materials which is composed by the intergrowth of different polymorphs, i.e., polymorphs A, B, and C [15]. Up to now, a variety of catalytic applications have been successful due to the 3-dimensionally interconnected large pore networks and strong acidity of this zeolite. Furthermore, the high density of defects originating from the intergrowth of different polymorphs are advantageous for the generation of Lewis acid sites, which is favorable for the conversion of carbohydrates [16,17]. Tatsumi et al. reported the effective generation of Lewis acid sits on low silica beta zeolite by high temperature calcination [17,18]. Since the first trial of Sn-beta zeolite for glucose conversion by Davis et al., numerous studies have followed on the synthesis and application of these stannosilicate zeolites [19,20]. Beside the bottom-up hydrothermal synthesis of Sn-beta, various post-synthetic routes, including the acid dealumination of beta zeolite and subsequent Sn grafting through the solution mediated implantation, vapor phase, and solid-state implantation, were developed [21-24].

In the present study, Brönsted and Lewis bi-acidic SnAl-beta zeolites were successfully synthesized using the simple top-down isomorphic substitution of Sn on the dealuminated H-beta zeolite. The ratio of Brönsted acid/Lewis acid was finely regulated by employing different acid dealumination conditions (i.e., acid concentration and treatment time). The relative ratio of Brönsted and Lewis acid concentrations on the catalysts was characterized by infrared (IR) spectroscopy with adsorbed pyridine and correlated with the selectivity to fructose, 5-HMF, and levulinic+formic acids during the cascade conversion of glucose.

EXPERIMENTAL

1. Catalyst Preparation

H-beta was obtained by the calcination of commercial NH_4-beta (Zeolyst CP 814E, SiO_2/Al_2O_3=25) at 550 °C for 2 h. Dealuminated H-beta zeolites with varying Si/Al ratios were obtained by aluminum leaching with nitric acid aqueous solutions with different molarity (1-13 M) and treatment time (1-24 h). Generally, 1.0 g zeolite powder was immersed into the 20 ml nitric acid aqueous solution and refluxed at 100 °C for different periods. The treated sample was recovered by filtration with deionized (DI) water until the pH of the filtrate was ca. 7.0, and dried at 60 °C overnight. Finally, the sample was calcined at 550 °C for 4 h under flowing air. The dealuminated beta zeolite samples were denoted as deAl-beta-*x,y*, where *x* and *y* are the molarity of acid concentration and treatment time, respectively.

Sn-containing deAl-beta zeolites with different Sn content were prepared by isomorphic substitution of Sn into the deAl-beta zeolites. Generally, 1.0 g deAl-beta zeolite was immersed in the 100 ml isopropyl alcohol containing 27 mmol $SnCl_4 \cdot 5H_2O$ and refluxed at 80 °C for 6 h under N_2 atmosphere. The treated sample was recovered by filtration with excess isopropyl alcohol and dried at 60 °C overnight. The sample was finally calcined at 200 °C for 6 h and consecutively 550 °C for 6 h with ramping rate of 3 °C min^{-1} under flowing air. The Sn incorporated beta zeolites were denoted as SnAl-beta-*x,y*, where *x* and *y* are the molarity of acid concentration and treatment time, respectively.

2. Characterization

The crystallinity of catalysts was determined by powder X-ray diffraction (XRD) using a Rigaku SmartLab X-ray diffractometer with Cu-Kα radiation in the 2θ range of 3-50° (scan rate=4° min^{-1}). The relative crystallinity of the deAl- and SnAl-beta zeolites was determined by comparing the areas of the intense X-ray peak around 2θ=22.5°, corresponding to the (302) reflection of the *BEA structure, with that of H-beta. Elemental analysis for Al, Si, and Sn was carried out on a PerkinElmer OPTIMA 7300DV inductively coupled plasma spectrometer. The textural property of catalysts was measured by N_2 sorption experiments on a Micromeritics Tristar II analyzer. UV-diffuse reflectance spectroscopy (DRS) was measured on a Shimadzu UV-2600 UV-Vis spectrophotometer. The UV absorption spectra were plotted using the Kubelka-Munk function. X-ray photoelectron spectroscopy (XPS) was performed on a PHI 5000 Versa Probe II with Al-Kα radiation ($h\nu$=1,486.6 eV).

The acidic property of the solid samples was determined by IR spectroscopy using pyridine as a probe molecule. Pyridine adsorption-desorption measurements were carried out on self-supporting zeolite wafers of approximately 12 mg with 1.3 cm diameter activated under vacuum at 550 °C for 2 h inside a home-built IR cell with ZnSe windows. Prior to the adsorption of pyridine, the IR spectrum of hydroxyl region was recorded at 100 °C. Then, the sample was heated to 100 °C and saturated with excess pyridine (~1 kPa) for 0.5 h and subsequently purged with flowing N_2 (100 ml min^{-1}) for 1 h. The IR spectra were recorded on a Nicolet 6700 FT-IR spectrometer at 200 °C. The concentrations of Brönsted and Lewis acid sites were calculated from the intensity of the IR bands around 1,550 and 1,450 cm^{-1}, respectively, by using the extinction coefficients given by Emeis [25].

3. Catalysis

Catalysis was carried out with reference to the reaction conditions in the literature for the same reaction using a water solvent [26]. The glucose conversion was conducted in a 23 ml Teflon-lined

stainless autoclave reactor containing 1 g glucose, 10 g DI water, and 0.1 g catalyst at 160 °C and 100 rpm for 1-24 h under autogenous pressure. After a certain reaction time, the autoclave was rapidly cooled to room temperature. All the reaction products were syringe-filtered and diluted with DI water to analyze with high performance liquid chromatograph (Youngin Chromass YL9100 plus) equipped with refractive index and UV (280 nm) detectors and an Agilent Hi-Plex H column (300×7.7 mm). The mobile phase was 5 mM H_2SO_4 aqueous solution and the flow rate was 0.6 ml min^{-1} at a column temperature of 65 °C. All reactions were repeated twice or more to confirm the reproducibility. For comparison, some blank tests, i.e., a reaction under an aqueous solvent without a catalyst and a reaction under the 0.01 mM $SnCl_4$ aqueous solution, were also performed under the same reaction conditions. In addition, after 6 h of reaction, the used catalyst was recovered by filtration, washed repeatedly with excess water, and calcined at 550 °C for 6 h and then employed for the reusability test. The glucose conversion and the products selectivity were determined as follows.

Glucose conversion (%)
=(moles of reacted glucose/initial moles of glucose)×100

Product selectivity (%)
=(moles of product/moles of reacted glucose)×100

RESULTS AND DISCUSSION

1. Physicochemical Properties of Catalysts

Fig. 1 shows the powder XRD patterns of deAl-beta and SnAl-beta zeolites prepared under the different concentration of nitric acid. Although there are some changes in the crystallinity of zeolites, all the samples exhibit X-ray diffraction peaks of (101) and (302), which are the characteristic peaks of *BEA structure in spite of the acid dealumination with different acid concentration. As shown in Table 1, the relative crystallinity of the deAl-beta-7-24 was not reduced while that of SnAl-beta zeolites was decreased to 60-83% with respect to H-beta. It is interesting that a careful look at the XRD pattern of deAl-beta-7-24 shows a shift in the (302) peak toward the higher 2θ range compare to that of H-beta. This shift (Δ= 0.04°) indicates the contraction of the zeolite unit cell upon dealumination [27]. On the other hand, the (302) peak shift toward the lower 2θ range as the substituted amount of Sn increases, which is the evidence of unit cell expansion. This can be rationalized by the

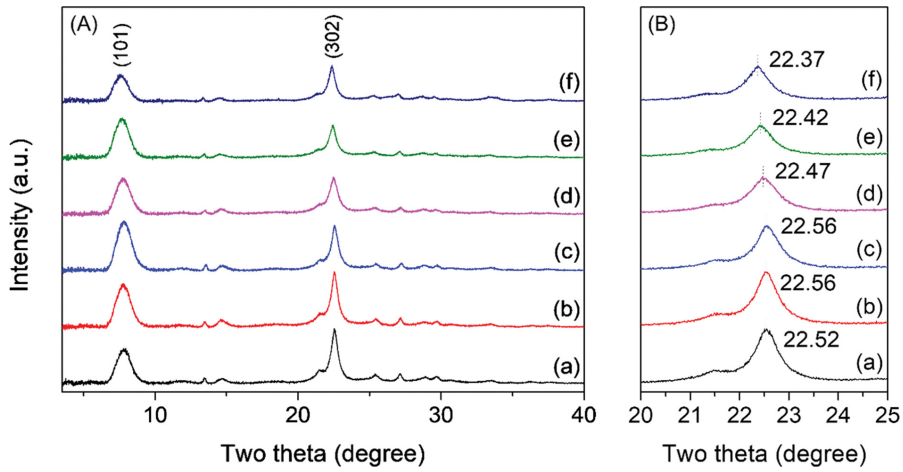

Fig. 1. (A) Powder XRD patterns of (a) H-beta, (b) deAl-beta-7-24, (c) SnAl-beta-1-24, (d) SnAl-beta-3-24, (e) SnAl-beta-7-24, and (f) SnAl-beta-13-24 and (B) each zoomed on the 2θ range of the (302) peak.

Table 1. Physicochemical properties of zeolite catalysts prepared in this study

Catalyst	Crystallinity (%)[a]	Si/Al[b]	Sn/Al[b]	BET surface area (m^2 g^{-1})[d]	Acid concentration (μmol g^{-1})[e]		L/(B+L)
					Brönsted	Lewis	
H-beta	100	12.5[c]	-	570	268	129	0.32
deAl-beta-7-24	100	864	-	510	5	36	0.88
SnAl-beta-1-24	83	256	1.9	500	32	46	0.59
SnAl-beta-3-24	66	263	2.9	490	16	52	0.76
SnAl-beta-7-24	60	623	4.9	530	8	65	0.89
SnAl-beta-13-24	65	1,418	21.3	440	8	85	0.91

[a]Determined by powder XRD
[b]Determined by elemental analysis, unless otherwise stated
[c]From the supplier's information
[d]Calculated from N_2 adsorption data
[e]Determined by the IR spectroscopy with pyridine adsorption

larger covalent radius of Sn (1.41 Å) than Al (1.18 Å). Furthermore, the X-ray peaks for the SnO_2 phase at 2θ=26.7° (110), 34.0° (101), and 37.8° (200) were not observed over the SnAl-beta zeolites even after the final air calcination step in their preparation [20,22], indicating most of Sn atoms incorporated well into the zeolite framework.

Table 1 summarizes the physicochemical properties of zeolite samples prepared in this study. It can be seen that the Si/Al ratios of deAl-beta and SnAl-beta were increased with higher molarity of nitric acid used in the acid dealumination process. For example, when 13 M nitric acid was used for dealumination of H-beta for 24 h, most of the Al was extracted from the zeolite framework resulting in the higher Si/Al ratio than 1400. On the other hand, the Sn/Al ratios of SnAl-beta zeolites were increased as the higher concentration of nitric acid used for dealumination, because the isomorphic substitution of Sn starts from the defect sites on dealuminated sites, such as silanol nest [28]. Although the BET surface areas of deAl-beta and SnAl-beta were reduced compared to that (570 m^2 g^{-1}) of H-beta zeolite after acid dealumination, they still retained high surface areas higher than 440 m^2 g^{-1}, indicating the remarkable stability of *BEA structure. Roberge and coworkers reported that the structure of commercial beta zeolite is resistant to the attack of nitric acid with concentrations up to 6 M with only minor structural collapse [29]. Also, acid leaching with nitric acid concentrations higher than 1 M selectively removes framework aluminium, especially located near to structural defects and on the external surface regions. In addition, acid leaching with lower concentration than 1 M hydrochloric acid mainly extracts the extra framework aluminum which is not suitable for the isomorphic substitution of metals. Thus, all the SnAl-beta zeolites prepared in this study may have framework Sn species. However, the Si/Sn ratios (67-135) of all the SnAl-beta zeolites were considerably higher than 12.5, indicating that Sn was grafted only to some dealuminated sites.

The presence of framework Sn species was further confirmed by UV-DRS technique shown in Fig. 2. For the H-beta, there were only weak UV absorption bands for Al components at 230-240 nm and 270-280 nm, which are corresponding to tetrahedral and octahedral Al sites, respectively [30]. Since such Al bands were not observed in the deAl-beta-7-24 sample, it can be also confirmed that dealumination by acid treatment occurred efficiently. On the other hand, the UV absorption bands centered at around 219, 250, and 265 nm can be assigned to tetrahedrally-coordinated framework Sn sites, small SnO_2 domains, and bulk SnO_2 particles, respectively [31]. The intensity of both tetrahedrally-coordinated Sn and SnO_2 particles for SnAl-beta zeolites was increased as the higher concentration of nitric acid used for dealumination, i.e., with the higher Sn/Al ratios (Table 1). Although, the higher the Sn content, the higher the UV absorption bands were observed at 250 and 265 nm, these SnO_2 particles were not additionally observed from their XRD analysis as described above (Fig. 1).

Fig. 3 shows the Sn 3d XPS results for the H-beta, deAl-beta-7-24, and the four SnAl-beta zeolites prepared in this study. Unlike the H-beta and deAl-beta-7-24, all the four Sn treated zeolites showed two types of XPS spectra, i.e., Sn $3d_{5/2}$ and Sn $3d_{3/2}$ [22,32]. Here, the discussion is based on Sn $3d_{5/2}$, because Sn $3d_{3/2}$ shows the almost the same trend as all the catalysts. The Sn $3d_{5/2}$ XPS spectra can be classified into three types according to their binding energy, i.e., ca. 484.5, 486.5, and 487.5 eV for the metallic Sn^0, SnO_2, and tetrahedral Sn species in the zeolite framework, respectively [22,32]. As shown in Fig. 3, only the tetrahedral Sn species was detected for all the SnAl-beta zeolites, which also indicates most of the Sn incorporated well into the zeolite framework.

It is well known that the tetrahedral Al residing in zeolite framework acts as the Brönsted acid, and the dealumination by acid

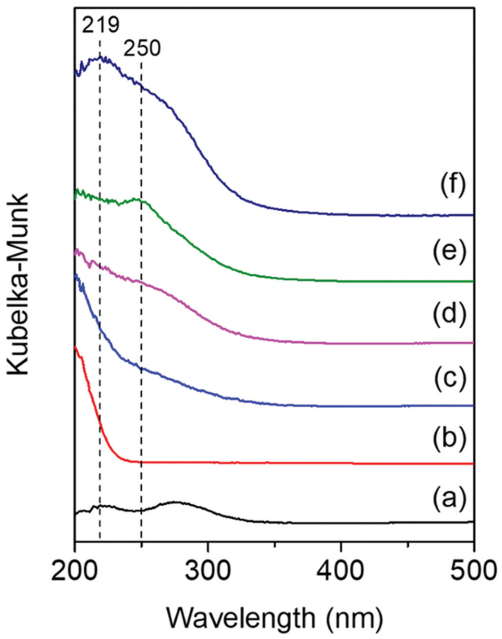

Fig. 2. UV-DRS spectra of (a) H-beta, (b) deAl-beta-7-24, (c) SnAl-beta-1-24, (d) SnAl-beta-3-24, (e) SnAl-beta-7-24, and (f) SnAl-beta-13-24.

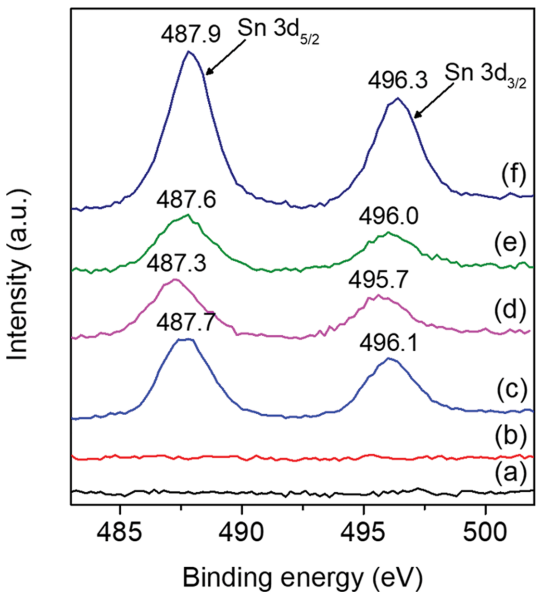

Fig. 3. Sn 3d XPS spectra of (a) H-beta, (b) deAl-beta-7-24, (c) SnAl-beta-1-24, (d) SnAl-beta-3-24, (e) SnAl-beta-7-24, and (f) SnAl-beta-13-24.

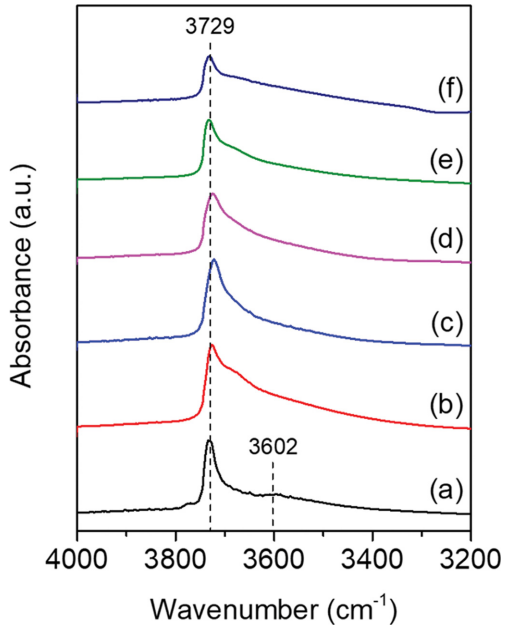

Fig. 4. IR spectra in the 3,200-4,000 cm^{-1} region of (a) H-beta, (b) deAl-beta-7-24, (c) SnAl-beta-1-24, (d) SnAl-beta-3-24, (e) SnAl-beta-7-24, and (f) SnAl-beta-13-24.

leaching and the incorporation of Sn generally modify the acidic properties of zeolite catalysts [19,20]. As a result of acid dealumination, the concentration of Brönsted acid (Si-OH-Al) sites in zeolite was decreased as the Al broke away from the framework. This can be demonstrated by the reduction of 3,600 cm^{-1} band (Si-OH-Al) in the IR spectra of deAl-beta and SnAl-beta zeolites shown in Fig. 4 [33]. Also, the intensity of the band around 3,730 cm^{-1}, which is corresponding to the OH stretching vibrations of silanols (Si-OH), was reduced as the amount of framework Sn increased [33]. This implies that the incorporation of Sn preferably occurs on the silanol nest, which is generated by the Al leaching from the zeolite framework.

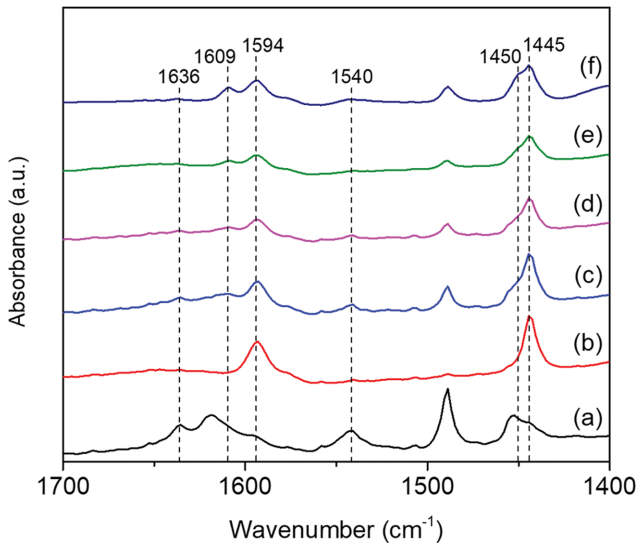

Fig. 5. Pyridine-adsorbed IR spectra of (a) H-beta, (b) deAl-beta-7-24, (c) SnAl-beta-1-24, (d) SnAl-beta-3-24, (e) SnAl-beta-7-24, and (f) SnAl-beta-13-24.

The changes in Brönsted and Lewis acid site concentrations were quantitatively analyzed by IR spectroscopy with adsorbed pyridine (Fig. 5). The IR bands centered at 1,540 and 1,636 cm^{-1} can be assigned to the C-N stretching vibration of pyridinium ion adsorbed on the Brönsted acid sites, while the bands at 1,450 and 1,609 cm^{-1} correspond to the pyridine interacting with the Lewis acid sites (i.e., isolated Sn sites) in the zeolite framework [33]. Also, the bands at 1,445 and 1,594 cm^{-1} can be assignable to the hydrogen-bonds between pyridine and the surface silanol groups of zeolite [34]. As shown in Fig. 5, all bands corresponding to the Brönsted and Lewis acids disappeared after dealumination, and the bands (1,445 and 1,594 cm^{-1}) related to the pyridine adsorbed on the surface silanols were significantly increased on the deAl-beta-7-24, indicating the formation of silanol nest on the dealuminated zeolite framework. This is also well correlated with the increase of IR band at 3,729 cm^{-1}, corresponding to the surface silanols over deAl-beta-7-24 shown in Fig. 4.

We should note here that the intensity of the pyridine on the surface silanols at 1,445 and 1,594 cm^{-1} over SnAl-beta-7-24 decreased when compared to that of deAl-beta-7-24, and instead the two IR bands at 1,450 and 1,609 cm^{-1} were increased again by the isomorphic substitution of Sn (Fig. 5). This clearly shows the formation of Lewis acid sites by Sn. Also, the bands corresponding to the Lewis acid sites were increased over SnAl-beta zeolites with the higher concentration of nitric acid used, which is coincident with the increase of Sn/Al ratios over these zeolites shown in Table 1. However, the intensity of IR bands related to the Brönsted acid sites (1,540 and 1,636 cm^{-1}) was continuously reduced with dealumination and Sn substitution. This implies that the ratio of Brönsted acid/Lewis acid concentration can be effectively controlled by the acid dealumination conditions.

2. Cascade Conversion of Glucose to 5-HMF

The catalytic conversion of glucose was investigated at 160 °C over the beta zeolites with different acidic properties. As shown in Fig. 6, H-beta exhibits moderate conversion of glucose while deAl-beta-7-24 shows very slow conversion, which is the similar to the case without using catalyst. However, the conversion of glucose was significantly increased and reached higher than 70% within 2 h when Sn was introduced on the frameworks of beta zeolite (SnAl-beta-7-24). Also, the yield of 5-HMF over this Sn-containing zeolite catalyst was rapidly increased from the onset of reaction and reached the highest value (20%) after 6 h of reaction. After that, the glucose conversion seemed to gradually approach the thermodynamic equilibrium at the reaction temperature. Since the reaction in 0.01 mM $SnCl_4$ aqueous solution, which is similar to the Sn concentration of SnAl-beta-7-24, showed much lower activity than SnAl-beta-7-24, the possibility of reaction by Sn leached from zeolite framework can be excluded. These results indicate that the glucose activation over the Sn-derived Lewis acid site is the most important factor in this cascade reaction. Although H-beta has much stronger pyridine interacting IR bands for Lewis acid sites (Fig. 5 and Table 1), the glucose conversion and 5-HMF yield were lower than those of SnAl-beta-7-24. This implies that the Sn-derived Lewis acid site is more effective in glucose conversion than

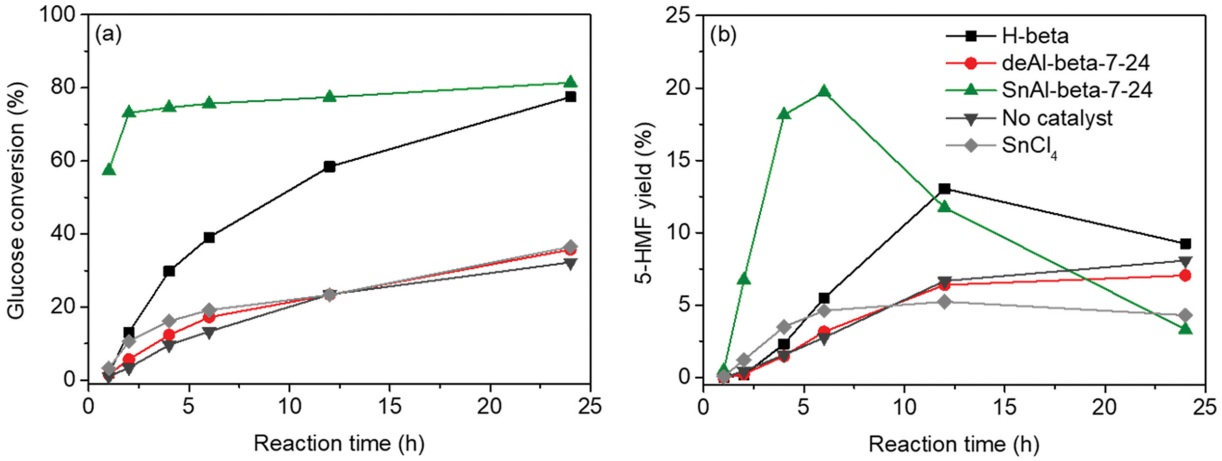

Fig. 6. (a) Glucose conversion and (b) 5-HMF yield over H-beta (■), deAl-beta-7-24 (●), and SnAl-beta-7-24 (▲) at 160 °C. For comparison, the glucose conversion and 5-HMF yield with no catalyst (▼) and 0.01 mM $SnCl_4$ (◆) were also added.

that intrinsically existing in H-beta [32,34,35]. It is well known that the Lewis acid sites generated from the calcination to make a zeolitic acid catalyst change to the Brönsted acid sites under the aqueous condition.

Considering the reaction on the aqueous solution giving much lower selectivity to 5-HMF compared to other polar organic solvents (e.g., 1-allyl-3-methylimidazolium chloride, dimethyl sulfoxide, methyl isobutyl ketone, dimethyl formamide, etc.), the yield of 5-HMF over the SnAl-beta-7-24 catalyst is remarkable [36]. In general, when water was used as a solvent, the yield of 5-HMF over H-beta was ca. 3-15% [32,34,35], which is similar to the result of this study. However, the yield of 5-HMF decreased after 6 h of reaction due to the further hydration to levulinic and formic acids (Scheme 1), and furthermore the other side reactions such as con-

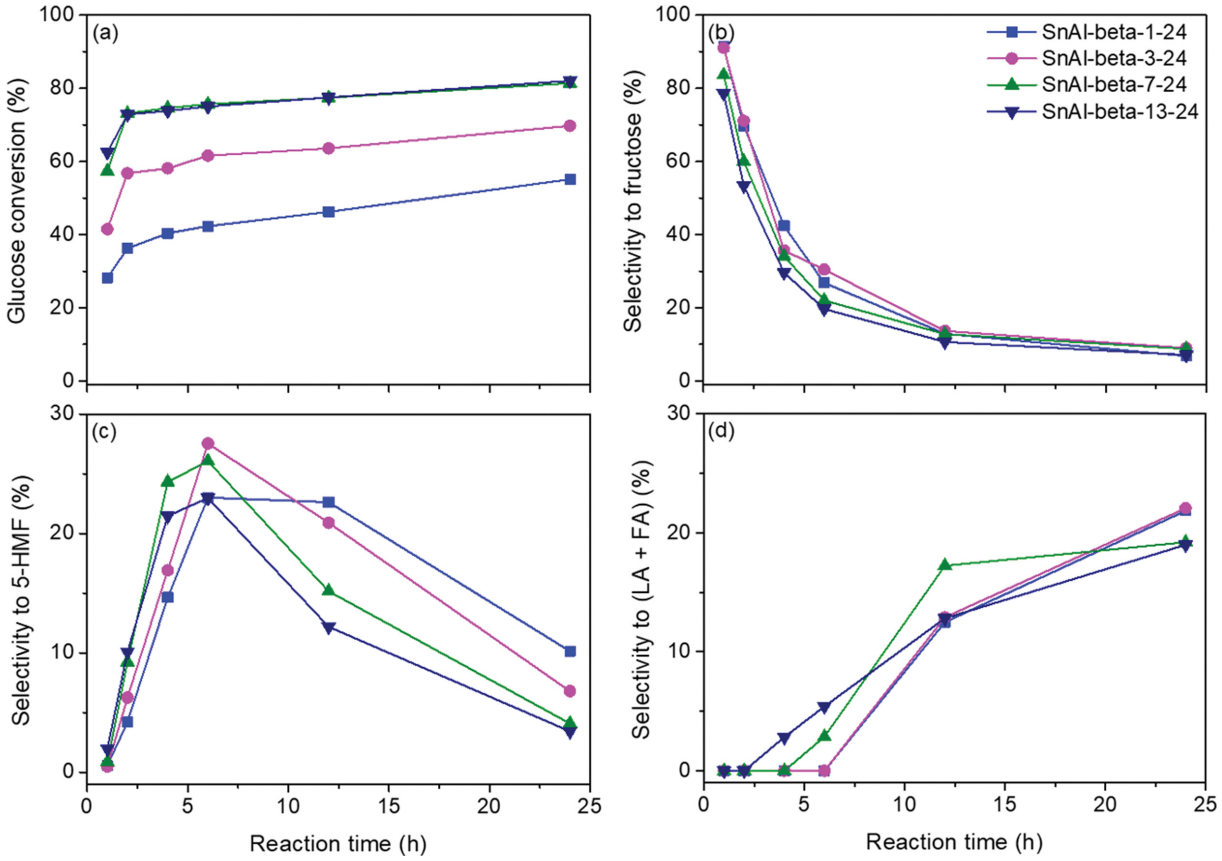

Fig. 7. (a) Glucose conversion and selectivity to (b) fructose, (c) 5-HMF, and (d) levulinic+formic acids over SnAl-beta-1-24 (■), SnAl-beta-3-24 (●), SnAl-beta-7-24 (▲), and SnAl-beta-13-24 (▼) at 160 °C.

densation to macromolecular substances like humin under the acidic environment [37]. On the other hand, this rapid decrease of 5-HMF yield with extended reaction time was hardly observed on the reactions with no catalyst and over the deAl-beta-7-24.

Fig. 7 shows the glucose conversion and selectivity to the major products (i.e., fructose, 5-HMF, and levulinic acid+formic acid) at 160 °C over SnAl-beta zeolites synthesized by acid dealumination with different concentration of nitric acid. The initial conversion of glucose increased in the order of SnAl-beta-1-24<SnAl-beta-3-24< SnAl-beta-7-24<SnAl-beta-13-24, indicating that the higher Lewis acid concentration is favored for this reaction. However, the conversion of glucose over SnAl-beta-7-24 and SnAl-beta-13-24 was almost identical after 2 h of reaction. This is probably due to the presence of thermodynamic equilibrium between glucose and fructose at the reaction temperature studied here [38,39]. As shown in Figs. 7(b)-(d), on the other hand, fructose is the prevailing product over all the SnAl-beta catalysts at the onset of reaction which is produced by the isomerization of glucose over Lewis acid sites (Scheme 1). The selectivity to fructose over SnAl-beta zeolites was inversely proportional to the glucose conversion due to the secondary conversion of fructose to 5-HMF. Thus, the selectivity to fructose continuously decreased from the onset of the reaction and 5-HMF became a dominating product after 6 h of reaction indicating the occurrence of Brönsted acid catalyzed dehydration of fructose (Scheme 1). SnAl-beta-3-24 exhibits the highest selectivity to 5-HMF, despite the relatively lower concentration of its total acid sites than those of SnAl-beta-7-24 and SnAl-beta-13-24. As shown in Fig. 7(d), however, the higher concentration of acid sites on SnAl-beta-7-24 and SnAl-beta-13-24 facilitates the further hydration of 5-HMF to levulinic and formic acids, resulting in the lower selectivity to 5-HMF.

As shown in Fig. 8, the longer periods of dealumination also had a positive effect on the glucose conversion and 5-HMF yield. SnAl-beta-7-24, prepared by the dealumination with 7 M nitric acid for 24 h, exhibits the highest initial conversion and 5-HMF yield among the SnAl-beta-7 catalysts. This is probably due to the balanced activity of both Brönsted and Lewis acid sites on this catalyst. When the SnAl-beta-7-24 catalyst was reacted for 6 h (1 cycle), and consecutively the reacted sample was regenerated by calcination at 550 °C for 6 h and tested again under the same reaction

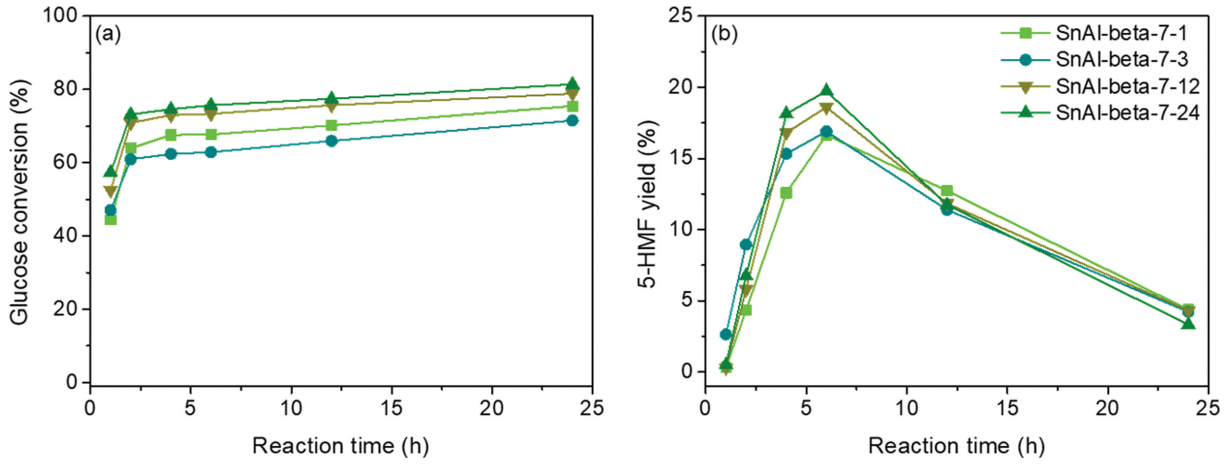

Fig. 8. (a) Glucose conversion and (b) 5-HMF yield over SnAl-beta-7-1 (■), SnAl-beta-7-3 (●), SnAl-beta-7-12 (▲), and SnAl-beta-7-24 (▼) at 160 °C.

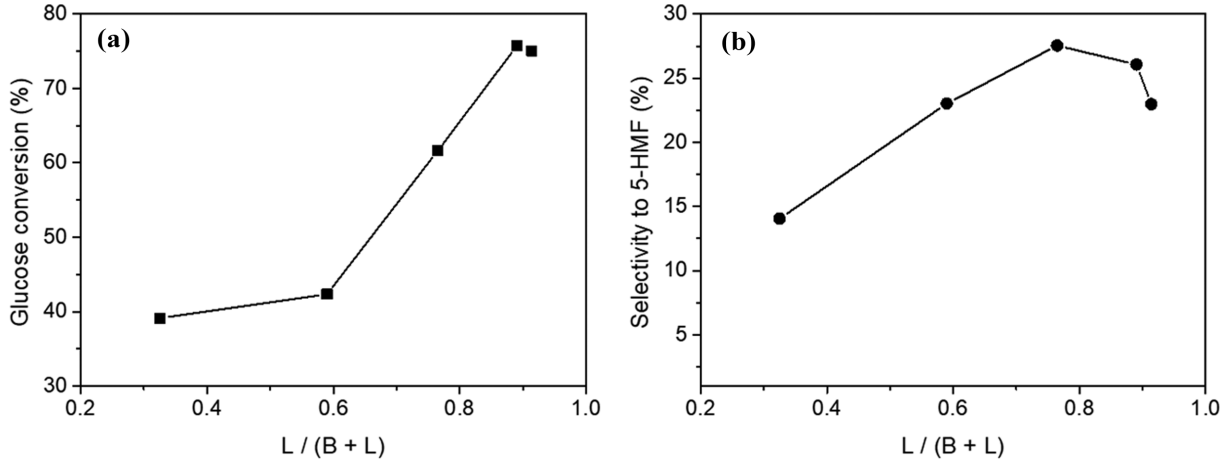

Fig. 9. (a) Glucose conversion and (b) selectivity to 5-HMF obtained at 160 °C as a function of Lewis acid portion over total acid concentration.

conditions (2 cycles), the glucose conversion and 5-HMF selectivity decreased by 21 and 7%, respectively, compared to that obtained from the first run (Fig. S1(a)). Since the powder XRD pattern of the 2 cycle catalyst was not much different from that of the fresh catalyst (Fig. S1(b)), it can be seen that the zeolitic phase was maintained, but the Sn active sites were affected by the calcined regeneration process.

Fig. 9 shows the glucose conversion and selectivity to 5-HMF with respect to the relative portion of Lewis acid over total acid concentration (i.e., L/(B+L)). The glucose conversion was increased until the portion of Lewis acid sites reached ca. 0.89 and further increase of this acid did not improve the catalytic activity, probably due to the limitation by thermodynamic equilibrium. However, the selectivity to 5-HMF reached its maximum at a certain point. The decrease of 5-HMF selectivity was observed over all the catalysts having Lewis acid portion higher than 0.76, which may be due to the lower activity of fructose dehydration over Brönsted acid sites and the further hydration of 5-HMF to levulinic and formic acids. From the overall results of this study, the optimized acidic properties of catalysts can be derived which can be applied fundamentally for the development of 5-HMF production technology.

CONCLUSIONS

The bi-acidic SnAl-beta zeolites with different Brönsted and Lewis acidity were successfully prepared by dealumination with nitric acid and isomorphic substitution of Sn. The ratio of Lewis/Brönsted acidity of SnAl-beta zeolites was controlled by adjusting the degree of dealumination, which was achieved by the acid concentration and treatment period. As a result, the higher the nitric acid concentration, the higher the Lewis acid concentration of catalysts. The successful substitution of Al by Sn was demonstrated by UV-DRS, and the acid concentration of catalysts was quantified by IR spectroscopy with adsorbed pyridine. The cascade conversion of glucose to 5-HMF over SnAl-beta zeolites was strongly influenced by its acidic property. The conversion of glucose was proportional to the Lewis acid portion in the catalyst up to 0.89 and leveled off at the higher portion, probably due to the thermodynamic limitation. The selectivity to 5-HMF reached its maximum when the portion of Lewis acid site in catalyst was 0.76, because both Brönsted and Lewis acids are required for the cascade conversion of glucose to 5-HMF. From the overall results of this study, the optimal acidic properties of catalysts for the development of 5-HMF can be suggested.

ACKNOWLEDGEMENT

This work was supported by the Incheon National University Research Grant in 2017.

SUPPORTING INFORMATION

Additional information as noted in the text. This information is available via the Internet at http://www.springer.com/chemistry/journal/11814.

REFERENCES

1. J. J. Bozell and G. R. Petersen, *Green Chem.*, **12**, 539 (2010).
2. C. Chatterjee, F. Pong and A. Sen, *Green Chem.*, **17**, 40 (2015).
3. W. Wei and S. Wu, *Fuel*, **225**, 311 (2018).
4. J. Esteban, P. Yustos and M. Ladero, *Catalysts*, **8**, 637 (2018).
5. A. Takagaki, *Catalysts*, **9**, 907 (2019).
6. J. Ji, Y. Xu, Y. Liu and Y. Zhang, *Catal. Commun.*, **144**, 106074 (2020).
7. M. Sajid, X. Zhao and D. Liu, *Green Chem.*, **20**, 5427 (2018).
8. Z. Xue, M.-G. Ma, Z. Li and T. Mu, *RSC Adv.*, **6**, 98874 (2016).
9. W. Zhang, Y. Zhu, H. Xu, M. Gaborieau, J. Huang and Y. Jiang, *Catal. Today*, **351**, 133 (2020).
10. H. Yan, Y. Yang, D. Tong, X. Xiang and C. Hu, *Catal. Commun.*, **351**, 1558 (2009).
11. N. H. Chung, V. T. Oanh, L. K. Thoa and P. H. Hoang, *Catal. Lett.*, **150**, 170 (2020).
12. T. D. Swift, H. Nguyen, Z. Erdman, J. S. Kruger, V. Nikolakis and D. G. Vlachos, *J. Catal.*, **333**, 149 (2016).
13. L. Hu, Z. Wu, J. Xu, Y. Sun, L. Lin and S. Liu, *Chem. Eng. J.*, **244**, 137 (2014).
14. Q. Xu, Z. Zhu, Y. Tian, J. Deng, J. Shi and Y. Fu, *Bioresources*, **9**, 303 (2014).
15. M. M. J. Treacy and J. M. Newsam, *Nature*, **332**, 249 (1988).
16. P. A. Wright, W. Zhou, J. Pérez-Pariente and M. Arranz, *J. Am. Chem. Soc.*, **127**, 494 (2005).
17. R. Otomo, T. Tatsumi and T. Yokoi, *Catal. Sci. Technol.*, **5**, 4001 (2015).
18. R. Otomo, T. Yokoi and T. Tatsumi, *ChemCatChem*, **7**, 4180 (2015).
19. M. Moliner, Y. Román-Leshkov and M. E. Davis, *Proc. Natl. Acad. Sci.*, **107**, 6164 (2010).
20. R. Bermejo-Deval, R. Gounder and M. E. Davis, *ACS Catal.*, **2**, 2705 (2012).
21. C. Hammond, S. Conarad and I. Hermans, *Angew. Chem. Int. Ed.*, **51**, 11736 (2012).
22. B. Tang, W. Dai, G. Wu, N. Guan, L. Li and M. Hunger, *ACS Catal.*, **4**, 2801 (2014).
23. J. Jin, X. Ye, Y. Li, Y. Wang, L. Li, J. Gu, W. Zhao and J. Shi, *Dalton Trans.*, **43**, 8196 (2014).
24. X. Yang, Y. Liu, X. Li, J. Ren, L. Zhou, T. Lu and Y. Su, *ACS Sustainable Chem. Eng.*, **6**, 8256 (2018).
25. C. A. Emeis, *J. Catal.*, **141**, 347 (1993).
26. H. Xia, H. Hu, S. Xu, K. Xiao and S. Zuo, *Biomass Bioenergy*, **108**, 426 (2018).
27. A. Omegna, M. Vasic, J. A. van Bokhoven, G. Pirngruber and R. Prins, *Phys. Chem. Chem. Phys.*, **6**, 447 (2004).
28. M. Srasra, S. Delsarte and E. M. Gaigneaux, *J. Phys. Chem. C*, **114**, 4527 (2010).
29. D. M. Roberge, H. Hausmann and W. F. Hölderich, *Phys. Chem. Chem. Phys.*, **4**, 3128 (2002).
30. D. Esquivel, A. J. Cruz-Cabeza, C. Jiménez-Sanchidrián and F. J. Romero-Salguero, *Micropor. Mesopor. Mater.*, **179**, 30 (2013).
31. J. W. Harris, M. J. Cordon, J. R. Di Iorio, J. C. Vega-Vila, F. H. Ribeiro and R. Gounder, *J. Catal.*, **335**, 141 (2016).
32. K. Saenluang, A. Thivasasith, P. Dugkhuntod, P. Pornsetmetakul, S. Salakhum, S. Namuangruk and C. Wattanakit, *Catalysts*, **10**,

1249 (2020).
33. J. Deng, J. Liu, W. Song, Z. Zhao, L. Zhao, H. Zheng, A. C. Lee, Y. Chen and J. Liu, *RSC Adv.*, **7**, 7130 (2017).
34. W. Dong, Z. Shen, B. Peng, M. Gu, X. Zhou, B. Xiang and Y. Zhang, *Sci. Rep.*, **6**, 26713 (2016).
35. N. Candu, M. E. Fergani, M. Verziu, B. Cojocaru, B. Jurca, N. Apostol, C. Teodorscu, V. I. Parvulescru and S. M. Coman, *Catal. Today*, **325**, 109 (2019).
36. Q. Hou, M. Zhen, L. Liu, Y. Chen, F. Huang, S. Zhang, W. Li and M. Ju, *Appl. Catal. B: Environ.*, **224**, 183 (2018).
37. C. Antonetti, D. Licursi, S. Sulignati, G. Valentini and A. M. Galletti, *Catalysts*, **6**, 196 (2016).
38. S. Kumar, D. Nepak, S. K. Kansal and S. Elumalai, *RSC Adv.*, **8**, 30106 (2018).
39. I. Delidovich and R. Palkovits, *ChemSusChem*, **9**, 547 (2016).

Supporting Information

Cascade conversion of glucose to 5-hydroxymethylfurfural over Brönsted-Lewis bi-acidic SnAl-beta zeolites

Hyejin An[*], Sungjoon Kweon[*], Dong-Chang Kang[**], Chae-Ho Shin[**], Jeong F. Kim[*], Min Bum Park[*,†], and Hyung-Ki Min[*,†]**

*Department of Energy and Chemical Engineering, Incheon National University, Incheon 22012, Korea
**Department of Chemical Engineering, Chungbuk National University, Cheongju, Chungbuk 28644, Korea
***LOTTE Chemical Research Institute, Daejeon 34110, Korea
(*Received 14 November 2020 • Revised 1 January 2021 • Accepted 26 January 2021*)

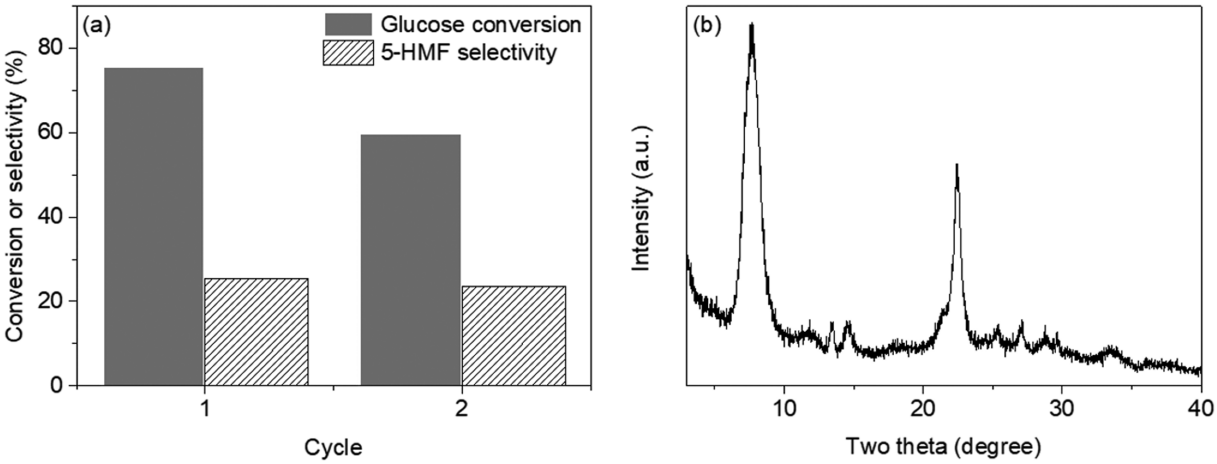

Fig. S1. (a) Glucose conversion and 5-HMF selectivity over SnAl-beta-7-24 at 160 °C for 6 h in the two consecutive runs and (b) powder XRD pattern of SnAl-beta-7-24 after two cycle runs.